PHYSICAL REVIEW B VOLUME 43, NUMBER 1 1 JANUARY 1991

Twin bands in martensites: Statics and dynamics

B. Horovitz
Department of Physics, Ben-Gurion University, P.O. Box 653, Beer-Sheva, 84105, Israel

G. R. Barsch
Materials Research Laboratory and Department of Physics, Pennsylvania State University, University Park, Pennsylvania, 16802

J. A. Krumhansl
Laboratory of Atomic and Solid State Physics, Cornell University, Ithaca, New York 14853
(Received 27 November 1989)

The theory of forming a coherent twin band and its relation to the parent-product interface in a martensitic transition is studied. We find that the twin band is stabilized by a long-range elastic interaction between the twin boundaries, which is mediated via the parent phase. The mean distance l between twin boundaries is then $l \sim \sqrt{L_2}$, with L_2 the size of a twin boundary, i.e., the product "grain" size. The collective twin-boundary oscillations ("dyadons") have unusually low frequencies and a limiting dispersion of frequency, which goes as the square root of the wave vector. Explicit results are given for a tetragonal-to-orthorhombic transition. We also show that dyadons cause the specific heat to change from a T^3 temperature dependence to T^2 at lower temperatures and to allow for a linear temperature dependence of the resistivity to extend to low temperatures. We compare our results with data on conventional martensites and on the more recent ceramic superconductors.

I. INTRODUCTION

Martensitic transitions form a unique class of phase transitions in the sense that a local free energy is not sufficient to describe them. A martensitic transition involves a structural transition whose transformation coordinate (or order parameter) is a lattice strain[1,2] $\sim \partial \mathbf{u}(\mathbf{r})/\partial \mathbf{r}$, with $\mathbf{u}$ the displacement of the center of mass of the unit cell at coordinate $\mathbf{r}$. A constant strain in the transformed lower-symmetry phase implies that $\mathbf{u}(\mathbf{r}) \sim \mathbf{r}$ is diverging with the size of the specimen and that the macroscopic boundary conditions of the crystal become involved. The resulting macroscopic changes, in some cases, are manifested by the so-called shape-memory effect.[3] In general, however, the bulk or macroscopic boundary conditions are fixed, and to relieve the above-mentioned real-space divergence, the system forms domains. This is the case if the martensitic phase is surrounded by an unstrained parent phase.

A key feature of a martensitic transition is then the formation of domains, inhomogeneities with structure on a scale much larger than the lattice constant. The crystallographic symmetry of the parent (untransformed) phase generally allows for formation of a few distinct variants or "twins" of the product (transformed) phase. A martensitic transition can then form a coherent array of twins such that the *average* strain on its boundaries vanishes. This then allows one to match the product phase with the parent phase, the crystal boundaries, or any other unstrained phase. The boundary at which this matching can occur is called an "invariant strain plane" or a habit plane.[2] This type of "twinning" martensite is the common form for low-strain structural transitions.

The coexistence of two twins results in a localized twin boundary. It has been shown[4–7] that a static solution for a twin boundary or for a periodic array of twin boundaries can be produced by a continuous displacive distortion of the parent phase without any need for dislocations. Explicit solutions were given in a continuum theory by allowing for both nonlinear elasticity and for nonlocal strains (i.e., strain gradients). The significance of this description, as will emerge below, is that large-scale motion at low frequency is allowed by the coherent twin structure. Note that this motion results from rearranging a displacement field, i.e., each atom moves by a distance usually much smaller than the lattice constant. This is very different from the dynamics of dislocations whose motion involves discontinuities in the strain field, motion of atomic vacancies, and hence drag and damping.

In the present work we study the energetics involved in the formation of a twin band in a host matrix, a study which was briefly described earlier.[8,9] While the fundamental reason for the occurrence of a twin lattice with a habit plane has been understood,[1,2] we are not aware of any quantitative studies of this phenomenon which account for the inherent nonlinearities.

In Sec. II we consider a parent-product interface and derive the parent displacive response to the nonlinear strains in the product twin band. This response is a long-range elastic field which provides an effective interaction between the twin boundaries and determines their equilibrium spacing. In Sec. III we consider the motion of twin boundaries, which results in a highly nonlocal response. We find the proper normal modes for these twin-boundary oscillations—the dyadons[10]—and their spectrum.

In Sec. IV we study some physical observables which can probe dyadons. These include elastic vibrations and waves, scattering experiments, specific heat, and, via electron-dyadon coupling, a contribution to the resistivity. In the Appendixes we consider the explicit case of the tetragonal-to-orthorhombic transition. In Appendix A we derive the orientation of the habit plane and in Appendix B the static response of the parent (tetragonal) phase to the twin-boundary lattice in the product (orthorhombic) phase.

We note that the tetragonal-orthorhombic transition and related twin boundaries are of particular interest since they were observed in some of the copper oxide high-T_c superconductors.[11] In Sec. V we discuss some implications for the properties of these materials.

II. TWIN BOUNDARIES: STATICS

Structural transitions which lower the point-group symmetry can result in a few degenerate variants or twins. For example, the cubic-tetragonal (C-T) transition has three variants (by choosing each one out of three cube sides to change), while the tetragonal-orthorhombic (T-O) has two variants (by choosing either of two square sides to increase). The boundary between adjacent twins is called a twin boundary. Geometrical considerations determine the plane across which two twins are compatible;[2,12] for the C-T and T-O transitions twin boundaries are the $\{110\}$ planes.

Continuum models with nonlinear elasticity and with nonlocal strains (i.e., strain gradients) have been studied for the C-T and T-O transitions and static solutions of a twin boundary or a periodic array of twin boundaries have been found.[4–7] These solutions describe a continuous displacive distortion of the high-symmetry phase without any need for dislocations.

The local elastic free energy F in terms of an order parameter e (a strain component) has degenerate minima for the strain values corresponding to the allowed twins. Figure 1 shows the T-O case with minima at $e=\pm\epsilon/\sqrt{2}$, with e being the $\{110\}$ shear. A twin boundary is describable by a topological displacement soliton which interpolates (in space) between two degenerate minima. The continuum model then yields a one-dimensional solution $e(s)$ with $e(s\to\infty)=\epsilon/\sqrt{2}$ and $e(s\to-\infty)=-\epsilon/\sqrt{2}$, with s the space coordinate perpendicular to the twin boundary.

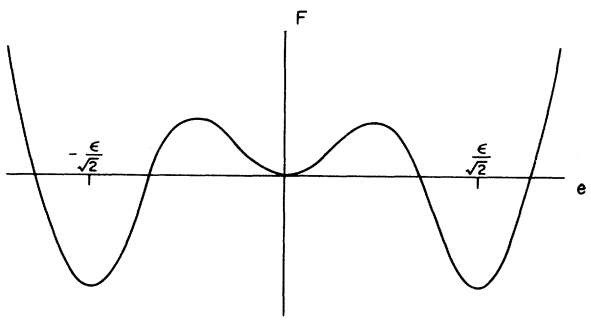

FIG. 1. Schematic form of a strain-dependent free energy. The degenerate minima at $\pm\epsilon/\sqrt{2}$ correspond to twins.

The total free energy is also minimized by periodic twin-boundary lattice (TBL) solutions whose periodicity $2l$ may lie in some finite range. In itself any one of these one-dimensional solutions does not determine a preferred value of l. In fact, since the absolute ground state is that of a homogeneous uniform strain, two adjacent twin boundaries can in principle annihilate each other and thereby reduce the total energy of the system. Hence these TBL solutions are unstable.

To account for the existence of TBL's we must introduce another phase coexisting with the product phase, e.g., a parent-product coexistence such that the interface is continuous with no loss of material. The parent product matching along a habit plane is then the raison d'être for the twin array. With only one variant on the product side the mismatch of lattice constants would increase the strain indefinitely along the habit plane. With a TBL, however, a habit plane can be found such that *average* lattice constants along the habit plane directions are equal on both sides of the interface. This then guarantees that all strains near the habit plane are finite and that dislocations can be avoided.

The construction of a habit plane[2,12] yields its orientation relative to the twin boundaries and also the thickness ratio of the two variants participating in the TBL. In Appendix A we derive the habit plane of a T-O transition. We find that, unlike in other structural transitions, there is a solution for any thickness ratio; the latter is then determined by dynamic or thermodynamic considerations.

The next step is to evaluate the interface energy, i.e., the amount of free energy stored in the elastic field fringing from the product into the parent phase. The geometry is illustrated in Fig. 2; the normal to the habit plane is in the x direction, and $x=0$ defines the habit plane. The intersection of the twin boundaries with the habit plane defines the $\hat{\mathbf{z}}$ direction (perpendicular to the plane of the figure), while the remaining perpendicular direction $\hat{\mathbf{y}}$ has an angle θ with the coordinate s along which the one-dimensional TBL modulation $\mathbf{u}(s)$ is defined.

We now face the problem of solving for the elastic displacement field $\mathbf{w}(x,y,z)$ in the parent phase $x<0$, with the boundary conditions

$$\mathbf{w}(x,y,z) \overset{x\to-\infty}{\to} 0 , \tag{1a}$$

and along the habit plane

$$\mathbf{w}(0,y=s/\cos\theta,z)=\mathbf{u}(s) . \tag{1b}$$

Consider first the situation far from the habit plane where $\mathbf{w}\to 0$ and linear elasticity should be valid. As argued below, this regime will give the dominant elastic energy. Linear elasticity then shows that the small displacement elastic normal modes have a wave vector $\mathbf{k}$, and their frequencies squared, ω^2, are proportional to the eigenvalues of the Christoffel tensor:

$$T_{im}=\sum_{j,l} C_{ijlm}k_j k_l , \tag{2}$$

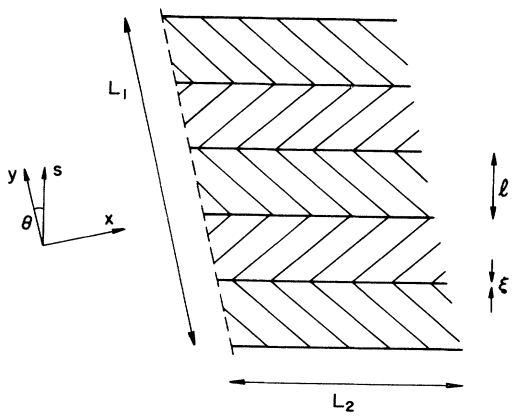

FIG. 2. Habit plane (dashed line) separates a twinned-product phase (on right) from the parent phase (on left). L_1, L_2, L_3 are dimensions of the product phase (L_3 is perpendicular to drawing). The separation between twin boundaries is l and their width is ξ. The direction s is perpendicular to the twin boundaries, x is perpendicular to the habit plane, z is the intersection of twin boundaries with the habit plane, and y is perpendicular to x and z.

where C_{ijlm} are elastic constants in the x,y,z coordinates of Fig. 2, which are not necessarily crystallographic symmetry axes. The local stability of the parent phase ensures that all the eigenvalues are $\omega^2>0$ for $\mathbf{k}$ real. Our static problem with no applied body forces requires the solution for $T_{ij}u_j=0$, i.e., $\det(T_{ij})=0$. The boundary condition (1b) implies that k_y is real, to allow for a periodic strain pattern along the y direction. Similarly, k_z is real; in fact, if y is a symmetry direction of the crystal a, z dependence is not generated and $k_z=0$. To allow for decay in the x direction [Eq. 1(a)], we must have an imaginary k_x with $\operatorname{Im}k_x<0$ so that $\mathbf{u}(\mathbf{k})\sim\exp(i\mathbf{k}\cdot\mathbf{r})\sim\exp[-(\operatorname{Im}k_x)x]\xrightarrow[x\to-\infty]{}0$. Such a solution can indeed satisfy $\det(T_{ij})=0$; in fact, the homogeneity of Eq. (2) implies the relation

$$k_x=-ia_jk_y,\quad \operatorname{Re}a_j>0\ , \tag{3}$$

where a_j depends on ratios of elastic constants C_{ijlm}. The number of solutions $\mathbf{w}^i$ satisfying (3) equals the dimensionality of $\mathbf{u}$, e.g., for a two-component field $j=1,2$. Since the boundary condition (1b) is a vector equation, a single solution is determined. We note that for $k_y=0$ the exponential decay should become a linear one; thus formally we exclude $k_y=0$ and consider only $|k_y|>2\pi/L_1$. The result (3) is derived explicitly for the *T-O* interface in Appendix B.

The solution in the parent phase, far from the habit plane, then has the form (suppressing the z dependence for simplicity)

$$\mathbf{w}(x,y)=\sum_{i,k_y}\mathbf{w}^i(k_y)e^{ik_yy+a_ik_yx}\quad(x<0)\ . \tag{4}$$

The remarkable feature of Eq. (4) is that the elastic field does not decay exponentially with $x<0$. The decay lengths $1/(a_ik_y)$ diverge as $k_y\to0$, and by expanding $\mathbf{w}^i(k_y)$ in powers of k_y it is seen that, in fact, $\mathbf{w}(x,y)$ decays as a power of $1/x$. Hence the fringing elastic field in the parent phase is of long range.

If Eq. (4) were valid at the habit plane, the boundary condition (1b) would yield

$$\sum_i\mathbf{w}^i(k_y)=\mathbf{u}(k_y/\cos\theta)\ , \tag{5}$$

where $\mathbf{u}(k)$ is the Fourier transform of $\mathbf{u}(s)$. We need, however, to account for the transition region near the habit plane which connects the nonlinear region of $\mathbf{u}(s)$ with the linear regime of Eq. (4). The thickness t of this transition region is either ξ, the width of a twin boundary which is a typical length scale for variations in the nonlinear field, or ϵl, which is the maximal displacement in each twin. In the following we assume $\xi\ll l$ and $\epsilon\ll1$ so that $t\ll l$. Hence $\mathbf{u}(x;k_y/\cos\theta)$ at $x=-t$ is needed in Eq. (5). By expanding in both k_y and x and noting that a $k_y=0$ component is not needed (uniform shift of the TBL), the lowest-order correction to (5) is $\sim k_yt$. In the following we mostly need $|k_y|<\pi/l$; hence $k_yt\ll1$ and (5) can be used.

The interface energy involves the elastic energy of the linear regime which has the form

$$E_{\text{in}}=\sum_{ijlm}\tfrac{1}{4}C_{ijlm}\int_{-\infty}^{-t}dx\int_{-\infty}^{\infty}dy\int_{-\infty}^{\infty}dz(\partial_iw_j+\partial_jw_i)(\partial_lw_m+\partial_mw_l)\ , \tag{6}$$

with $w_i(x,y)$ the components of $\mathbf{w}(x,y)$. By using Eq. (3) the derivatives give a k_y^2 dependence; however, the x integration involves

$$\int_{-\infty}^{t}dx\,\exp(2a_ik_yx)\sim k_y^{-1}\ .$$

Using Eq. (5), we obtain the general form of the interface energy as

$$E_{\text{in}}=L_1L_3\sum_{i,j}\alpha_{ij}\sum_k|k|u_i(k)u_j(-k)\ , \tag{7}$$

with α_{ij} of the order of elastic constants in the parent phase and dependent on the orientation angle θ of the habit plane. A typical term in (7) is $u_i(k)\simeq\epsilon l$, $k\sim1/l$, so that in the ground state we expect

$$E_{\text{in}}\simeq\alpha\epsilon^2L_1L_3l\ , \tag{8}$$

with $\alpha=0(\alpha_{ij})$; a more explicit derivation is given below.

We return now to the neglected transition region $-t<x<0$, which involves energy densities of order $\alpha\epsilon^2$ in a volume L_1L_3t. Since $t\ll l$, the dominant interface energy is that of the long-range elastic field, i.e., Eq. (8).

The elastic free energy within the product phase involves the creation energy per unit area E_0 of a twin boundary. Except very near the transition temperature, all terms in the (nonlinear) expansion of the free energy are comparable[5] so that $E_0\simeq\alpha\epsilon^2\xi$. This relation assumes

a proper ferroelastic material (i.e., strain is the primary order parameter); otherwise, E_0 depends primarily on the energies of a finite wave vector or optic-phonon mode which represents the primary order parameter. The free energy of a TBL solution can be separated into the free energy of $L_1\cos\theta/l=N_{\rm TB}$ independent twin boundaries, i.e., $E_0'L_1/l$ (with $E_0'=E_0\cos\theta$), and the remainder being classified as the "interaction" between twin boundaries. Since the twin-boundary strains are exponentially localized in a width ξ,[4-7] their mutual interaction for $l\gg\xi$ becomes of order $\exp(-l/\xi)$. Hence the static energy of forming a TBL is

$$E_{\rm TBL}=E_0'L_1L_2L_3/l[1+O(e^{-l/\xi})]\ . \tag{9}$$

The total l-dependent parent-product energy is the sum of Eqs. (8) and (9). Although Eq. (8) is a habit-plane (i.e., surface) energy, for all practical purposes it dominates over the bulk interaction energy in Eq. (9), i.e., $(\xi/l)\exp(-l/\xi)\ll l/L_2$; even for an extremely low value of[11] $l/\xi=10$ this implies $l/L_2\gg10^{-5}$ and with $l\simeq100$ Å one needs $L_2\ll10^7$ Å, consistent with typical grain sizes L_2 of order 1 μm.

Minimizing the sum of Eqs. (8) and (9) yields the optimal value of the TBL periodicity:

$$l\simeq[E_0'L_2/(\alpha\epsilon^2)]^{1/2}\simeq\sqrt{\xi L_2}\ . \tag{10}$$

This central result shows that the TBL is a finite-size effect and its periodicity increases with the size of the martensite inclusion, i.e., the grain size L_2. Note that E_0 and α are temperature dependent, and that close to the transition temperature or for improper ferroelastic martensites the second part of Eq. (10) does not hold. However, *all* other results below are valid for both proper and improper martensites. Equation (10) has been given previously[13] by phase-space arguments in Fourier space; however, the actual displacement field was not derived, and so it is not obvious whether that method contains our long-range effect.

We have analyzed data for twin bands resulting from a C-T transition in In-Tl.[14] The data show ten bands with L_2 in the range 2.7 to 10.5 μm and with l in the range 0.38 to 0.82 μm. A power law $l\sim(L_2)^\sigma$ is a reasonable fit (see Fig. 3) with $\sigma=0.4$–0.5. The ratio $l^2/L_2\simeq\xi$ is ~600 Å, implying fairly wide twin boundaries. Data on $YBa_2Cu_3O_x$ ($x=6.5$–7) show grain sizes of ~1 μm and twin bands related to a T-O transition with spacings of 200–1000 Å. The data show that l increases with L_2, but a quantitative analysis is not useful as the oxygen content is not well controlled. The ratio l^2/L_2 is on the atomic scale; high-resolution electron microscopy[11] has indeed shown very sharp twin boundaries with width within the unit cell. Thus the theory gives relationships between twin spacing l, grain size L_2, and twin-boundary thickness which are in reasonable agreement with experiment.

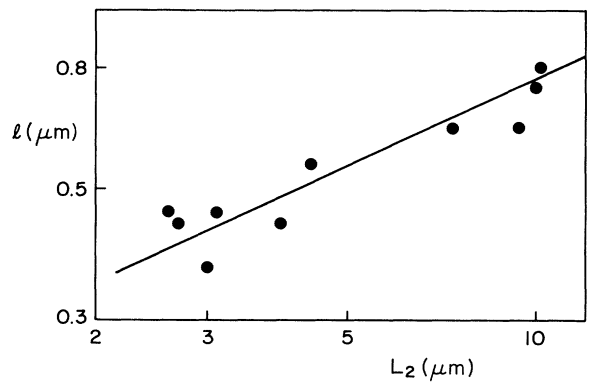

FIG. 3. Log-log plot of data on twin spacing l as function of twin-band size L_2 from Ref. 14. The line describes $l\sim\sqrt{L_2}$.

While the main physical features of a static TBL are contained in the above discussion, we present now an explicit form of a TBL and consider (i) a more quantitative analysis of the static energetics, (ii) general (nonperiodic) stacking, and (iii) the dynamic properties of the TBL. The explicit TBL form assumes (a) sharp twin boundaries, i.e., $l\gg\xi$, (b) a one-component field $u(s)$ to describe the TBL (e.g., the transverse displacement in the T-O system), and (c) strains equal but opposite in sign in alternating twins. The description is, however, fairly general in that it is independent of the details of the structural transition. If assumption (c) is relaxed, we expect some minor modifications, as mentioned below.

We define S_n ($n=0,1,\ldots,M$) to be collective coordinates for the location of each twin boundary in the s direction. The displacement field between S_{n-1} and S_n is $-(-1)^n\epsilon(s-S_{n-1})+u(S_{n-1})$, i.e.,

$$u(s)=\begin{cases}\epsilon(s-S_0)+\bar u, & S_0\le s\le S_1\ ,\\ -(-1)^n\epsilon(s-S_{n-1})-\sum_{j=1}^{n-1}(-1)^j\epsilon(S_j-S_{j-1})+\bar u, & S_{n-1}\le s\le S_n\ (n=2,3,\ldots,M)\ ,\end{cases} \tag{11}$$

with $\bar u=u(S_0)$ an overall shift. When all $S_n=nl$ these are equidistant twin boundaries; the form of $u(s)$ is then a periodic zigzag. We allow, however, S_n to vary from their expected positions and define displacement coordinates δ_n via

$$S_n=nl+\delta_n\ . \tag{12}$$

We further assume an even number M of twin boundaries with fixed overall length $S_M=S_0+Ml$ ($Ml=L_1\cos\theta$) and impose periodic boundary condition for $u(s)$, i.e., $u(S_M)=u(S_0)$. Equation (12) then implies $\delta_0=\delta_M$ and

$\sum_{n=1}^{M}(-1)^n\delta_n=0$. The values of l, $\bar{u}$, and δ_n are left as variational parameters which minimize the total elastic energy.

It is useful to evaluate the Fourier transform $u(q)$ of $u(s)$ with q values satisfying $\exp(iqMl)=1$. Since the $q=0$ term does not contribute to the energy [Eq. (7)] we evaluate $u(q)$ for $q\neq 0$, which after some algebra becomes

$$u(q)\equiv\int_{S_0}^{S_m}u(s)e^{-iqs}ds/Ml=-\frac{2\epsilon}{Ml}\sum_{n=1}^{M}\frac{(-1)^n}{q^2}e^{-iqnl-iq\delta_n}\ . \tag{13}$$

We next expand to second order in δ_n and Fourier transform $(-1)^n\delta_n=\sum_q\hat{\delta}(q)\exp(iqnl)$ with $|q|\leq\pi/l$ [the reason for the $(-1)^n$ becomes clear below] to obtain

$$u(q)=-\frac{2\epsilon}{l}\left[\sum_p\frac{l^2}{\pi^2(2p+1)^2}\delta_{q,\pi(2p+1)/l}-\frac{i}{q}\hat{\delta}(q')-\tfrac{1}{2}\sum_k\hat{\delta}(k)\hat{\delta}(q'-k)\right]\ . \tag{14}$$

Here p is an integer and $q'=q+2\pi p/l$, with p such that $|q'|<\pi/l$ in the second term or $|q'-k|<\pi/l$ in the third one, and $\delta_{k,q}$ a Kronecker δ function.

The interface energy [Eq. (7)] has then the form [to second order in $\hat{\delta}(q)$]

$$E_{\rm in}=\alpha L_1L_3\left[\frac{2\epsilon}{l}\right]^2\left[\sum_p\frac{l^3}{\pi^3|2p+1|^3}+\sum_q\sum_p\left[\frac{1}{|q+2\pi p/l|}-\frac{1}{|\pi(2p+1)/l|}\right]\hat{\delta}(q)\hat{\delta}(-q)\right]\ . \tag{15}$$

We note that the summation on p, in both terms, converges rapidly as p^{-3}. For example, $\sum_{p=0}^{\infty}(2p+1)^{-3}=1.05$, just 5% above the $p=0$ term. Hence the high-momenta components of (7) have a small effect, which *a posteriori* justifies the neglect of the transition region in evaluating the interface energy. We note also that there are no terms linear in $\hat{\delta}(q)$ and the coefficient of $\hat{\delta}(q)\hat{\delta}(-q)$ is positive. Hence the periodic TBL with $S_n=nl$ (i.e., $\delta_n=0$) is a configuration with minimum energy. For this case the energy is

$$E_{\rm in}^0=0.27\alpha\epsilon^2L_1L_3l\ , \tag{16}$$

which up to the numerical prefactor is the same as Eq. (8). The $l\sim\sqrt{L_2}$ relation Eq. (10) then follows with an additional prefactor of $(0.27)^{-1/2}=1.92$.

We note finally that the coefficient of $\hat{\delta}(q)\hat{\delta}(-q)$ in Eq. (15) diverges for $q\to 0$. As we show in Sec. III, when the proper normal modes are used, all restoring forces as well as the eigenfrequencies are finite.

III. TWIN BOUNDARIES: DYNAMICS

An analysis of the dynamics of twin boundaries yields a surprisingly nonlocal effect. To grasp the basic idea, first consider the motion of just one twin boundary as illustrated in Fig. 4. Since the strain $e(s)$ in the twins is fixed as $\pm\epsilon$, the displacement itself is nonlocal, $u(s)\sim\int_{S_m}^{s}ds'\,e(s')$. When one twin-boundary location S_m is shifted, the whole product phase with $s>S_m$ is displaced. Thus an apparently simple local motion of a boundary results in a coherent macroscopic motion.

To analyze this idea more precisely, we consider the kinetic energy of the TBL solution (11) with time-dependent collective coordinates $\delta_n(t)$ as dynamic variables. The kinetic energy, using Eq. (11), becomes

$$E_k=\tfrac{1}{2}\rho L_2L_3\int_{S_0}^{S_M}[\dot{u}(s)]^2ds$$

$$=\tfrac{1}{2}\rho L_2L_3\epsilon^2l\sum_{n=1}^{m}\dot{\eta}_n^2\ , \tag{17}$$

where ρ is the mass density, the overdot is $\partial/\partial t$, and a set of normal coordinates η_n, which we call dyadon modes,[10] are defined by the nonlocal transformation

$$\eta_1=\delta_0-\bar{u}\ ,$$

$$\eta_n=2\sum_{j=1}^{n-1}(-1)^j\delta_j+\delta_0-\bar{u}\quad(n=2,3,\ldots,M)\ . \tag{18}$$

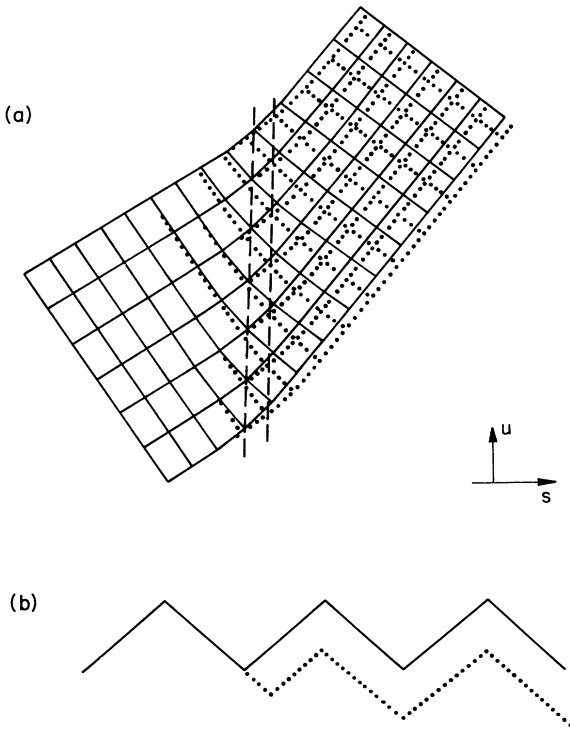

FIG. 4. Motion of a twin boundary. (a) Left (right) dashed line is a twin boundary separating the lattices with full (dotted) lines. Motion of the twin boundary results in displacing the *whole* lattice on the right from the full lines to the dotted ones. (b) Displacement field of a TBL $u(s)$ (solid line) and the effect of moving a single boundary as in (a) (dotted line).

Since δ_n form $M-1$ degrees of freedom [due to the constraint $\sum_{n=1}^{M}(-1)^n\delta_n=\hat{\delta}(q=0)=0$], the addition of the $\bar{u}$ coordinate allows η_n to form M degrees of freedom. Thus the Fourier transform $\eta(q)=\sum_{n=1}^{M}\eta_n \exp(iqnl)$ is related to $\hat{\delta}(q)$ by

$$\hat{\delta}(q)=\tfrac{1}{2}(e^{-iq}-1)\eta(q) \ . \tag{19}$$

Hence the $q\neq 0$ terms in the kinetic energy are $\sim \sum_q \hat{\delta}(q)/\sin^2(\frac{1}{2}ql)$, which shows a diverging kinetic mass as $q\to 0$ for the coordinates δ_n. This remarkable feature is a manifestation of the nonlocal effect of the twin-boundary motion, i.e., of the large-scale motion due to a boundary translation. Figure 5 shows this large-scale effect for $q\to 0$ as well as the effect on the strain field: adjacent boundaries move out of phase, while the displacement fields of adjacent twins are in phase. Another mode of interest is the one for $q=\pi/l$, shown in Fig. 6, which corresponds to a rigid translation of the TBL. Here adjacent boundaries move in phase, while the displacement field of adjacent twins are out of phase.

We proceed to find the spectrum of dyadons—the normal modes of TBL oscillations. The total effective Hamiltonian is composed of the sum of the elastic energy [Eq. (15)] and the kinetic energy [Eq. (17)]. The kinetic energy of the parent phase is neglected since it amounts to a surface term, while Eq. (17) is a bulk term for the kinetic energy. This is in contrast with the elastic energy whose bulk term is greatly reduced by the factor $\exp(-l/\xi)$ and therefore is dominated by the surface term, i.e., the response of the parent phase. More precisely, Eq. (4) yields for the kinetic energy of the parent phase

$$E_k^{\text{parent}} \simeq \tfrac{1}{2}\rho L_3 L_1 \sum_q |\dot{u}(q)|^2/q \ ,$$

which is small compared with (17) when $qL_2 \gg 1$. With this constraint we have then that the elastic energy is dominated by the parent phase, but the kinetic energy by the product phase.

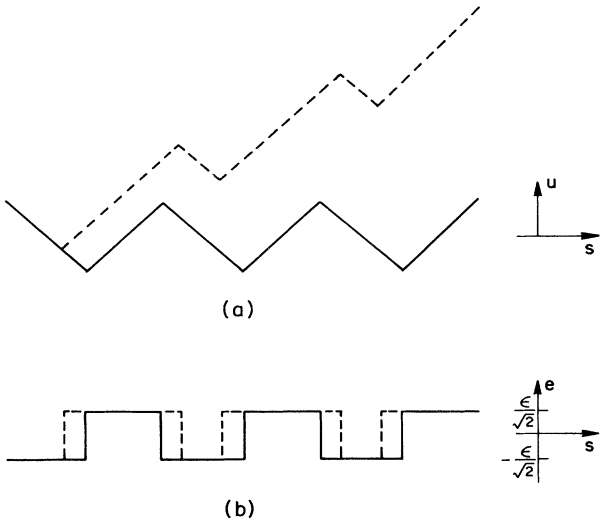

FIG. 5. $q\to 0$ modes: (a) Displacement field $u(s)$ of a TBL (solid line) and the effect of a $q\to 0$ dyadon (dashed line). (b) The strains $e(s)\sim \partial u/\partial s$ corresponding to (a).

This scenario has an analogy in a linear elasticity problem: Love waves[15] describe localized waves in a layer of material A with thickness L_2, which is attached to a bulk material B. When the elastic constant of material A is vanishing [to represent the $O(\exp(-l/\xi))$ term in Eq. (9)], the dispersion of Love waves is $\omega\sim\sqrt{q}$ for $|q|\gtrsim 1/L_2$; this has also been extended to anisotropic materials.[16]

By comparing Eq. (7) with Eq. (17) it seems as if $\omega\sim\sqrt{q}$ is obvious. However, Eq. (7) is the dominant restoring force only for the twin-boundary translation modes; hence we need to use the proper normal modes η_n. From Eqs. (15), (19), and (17) we obtain for the Hamiltonian, to second order in $\eta(q)$, with E_{in}^0 the static elastic energy,

$$\mathcal{H}=E_{\text{in}}^0+\tfrac{1}{2}\rho L_1 L_2 L_3 \epsilon^2 \sum_q [\dot{\eta}(q)\dot{\eta}(-q)+\omega_q^2\eta(q)\eta(-q)] \ , \tag{20}$$

and the dyadon eigenfrequencies are

$$\omega^2(q)=\omega_d^2 \sin^2(\tfrac{1}{2}ql) \sum_{p=-\infty}^{\infty} \left[\frac{1}{|ql/2\pi-p|} - \frac{1}{|\frac{1}{2}-p|} \right] \ , \tag{21}$$

and

$$\omega_d=[4\alpha/(\pi\rho l L_2)]^{1/2} \ . \tag{22}$$

Figure 7 shows the numerical evaluation of the dispersion curve [Eq. (21)]. For $q\to 0$, $\omega\sim\sqrt{q}$ as anticipated above; this square-root behavior is a manifestation of the long-range elastic force mediated through the parent phase. Note, however, that for $|q|L_2\leq 1$ the wavelength is longer than the size of the product phase, and parent-product distinction would be meaningless; the dispersion should then become linear, $\omega\sim q$. The $q\to 0$ mode is shown in Fig. 5; at $q=0$, $\eta(q)$ involves the $\bar{u}$ coordinate of Eq. (11), i.e., a uniform translation of the lattice in the direction of $\mathbf{u}$. Thus $\omega(q=0)=0$ would correspond to the translation symmetry of the whole system. Note that $q=0$ is not a uniform mode for δ_n [recall the unusual Fourier transform below Eq. (13)], but rather an antiparallel motion of the twin boundaries [Fig. 5(b)].

The spectrum (21) has a second zero mode at $q=\pi/l$,

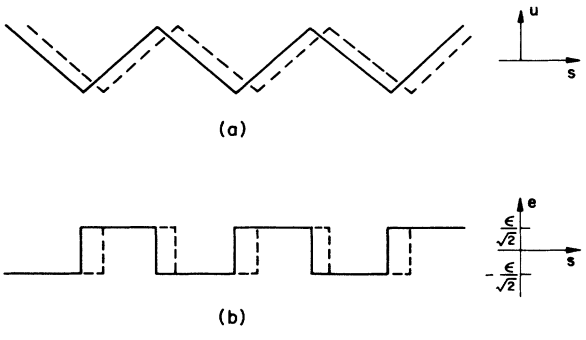

FIG. 6. $q=\pi/l$ mode: (a) Displacement field of a TBL (solid line) and the effect of a $q=\pi/l$ dyadon (dashed line). (b) The strain $e(s)\sim \partial u/\partial s$ corresponding to (a).

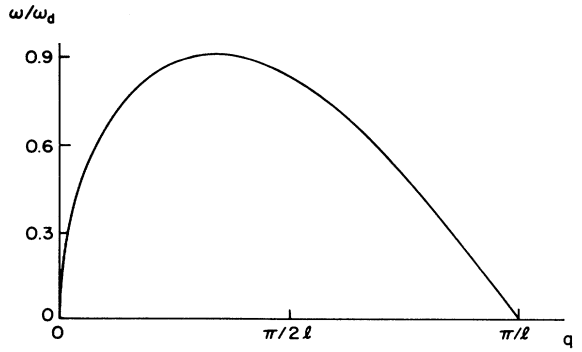

FIG. 7. Dispersion curve of dyadons [Eq. (21)].

which is approached linearly $\omega(q)=v_p|q-\pi/l|$ with $v_p=\omega_d l[7\zeta(3)/2]^{1/2}/\pi=2.05\omega_d l/\pi$. A $q=\pi/l$ mode corresponds to a uniform translation mode of the TBL, as shown in Fig. 6. Thus the modes near π/l are "phason"-type modes with v_p the phason velocity, relating to the translation invariance of the TBL energy in a continuum model. In practice, however, there are pinning forces due to either impurities or to lattice discreteness, the latter being important when the twin-boundary width ξ is short as compared with a lattice constant. These pinning effects can be represented as an additional term in the energy of the system which [unlike Eq. (7)] is local in the coordinate δ_n; hence

$$E_{\text{pin}}=\tfrac{1}{2}\beta\epsilon^2 L_2 L_3 \sum_n \delta_n^2$$

$$=\tfrac{1}{2}\beta\epsilon^2 L_2 L_3 M \sum_q \sin^2(\tfrac{1}{2}ql)\eta(q)\eta(-q)\ . \qquad (23)$$

The dispersion (21) is thus modified to

$$\omega_{\text{pin}}^2(q)=(\beta/\rho l)\sin^2(\tfrac{1}{2}ql)+\omega^2(q)\ . \qquad (24)$$

The $q\to 0$ form is not affected and $\omega_{\text{pin}}(q)\sim\sqrt{q}$. At $q=\pi/l$, however, $\omega_{\text{pin}}(q)=(\beta/\rho l)^{1/2}$ becomes finite.

The most remarkable feature of the dyadon spectrum is its extremely low-frequency values, on the order of the characteristic frequency ω_d. If ω_{ac} is a typical acoustic frequency at $q=\pi/l$ [$\omega_{\text{ac}}\simeq(\alpha/\rho)^{1/2}\pi/l$], then $\omega_d\simeq\omega_{\text{ac}}(l/L_2)^{1/2}$. The factor $(l/L_2)^{1/2}$ is small and the dependence on the grain size L_2 reminds us that the restoring force for the dyadon motion is an area-dependent interface and decreases (relative to the bulk kinetic energy) with increasing grain size. Using the l, L_2 values of Sec. II, we estimate ω_d of 10^9-10^{10} sec^{-1} in In-Tl, while $\omega_d\simeq 10^{10}-10^{11}$ sec^{-1} in $YBa_2Cu_3O_7$. In the latter compound we estimated a short ξ, and pinning effects can modify the actual frequencies as in Eq. (24). For In-Tl, however, we find a large ξ so that ω_d should be a realistic measure of the dyadon spectrum.

We note that these low-frequency modes constitute a rearrangement of the acoustic branch; i.e., the acoustic mode frequencies for $0<|q|<\pi/l$ collapse and form the dyadon spectrum. The rest of the acoustic branch at $|q|>\pi/l$ should be weakly affected by this rearrangement (Fig. 8); this results in a frequency gap of $\omega_d<\omega<\omega_{\text{ac}}$ at which the relevant sound modes cannot propagate in the direction perpendicular to the twin boundaries, analogous to a periodic interference filter in optics.

Note also that $\omega(q)\ll\omega_{\text{ac}}$ for all $|q|<\pi/l$. This inequality shows that the dyadon spectrum is well below that of other normal modes, a condition which is needed for the definition of translation modes as independent collective variables, as in other soliton-bearing theories.[7]

The periodicity of the static TBL is $2l$ so that the nominal Brillouin-zone boundary is at $\pm\pi/2l$. The spectrum in Fig. 7, however, has no gap at $\pi/2l$; this relates to a "glide line" symmetry (translation by l and reflection in u) so that the effective periodicity is l. For a more general TBL where the two twins have different strains $\epsilon_1\neq-\epsilon_2$ and hence different lengths l_1, l_2, the periodicity would be $2l=l_1+l_2$ and a gap would be present at $q=\pm\pi/2l$. The other peculiar features of the dyadon spectra, as discussed above, do not change for this more general situation.

We consider next a three-dimensional generalization of the dyadon concept. A twin-boundary motion is now modulated along a direction $\mathbf{r}$ ($\mathbf{r}\perp\mathbf{s}$) parallel to the twin boundary itself; i.e., the boundary is not flat anymore, but

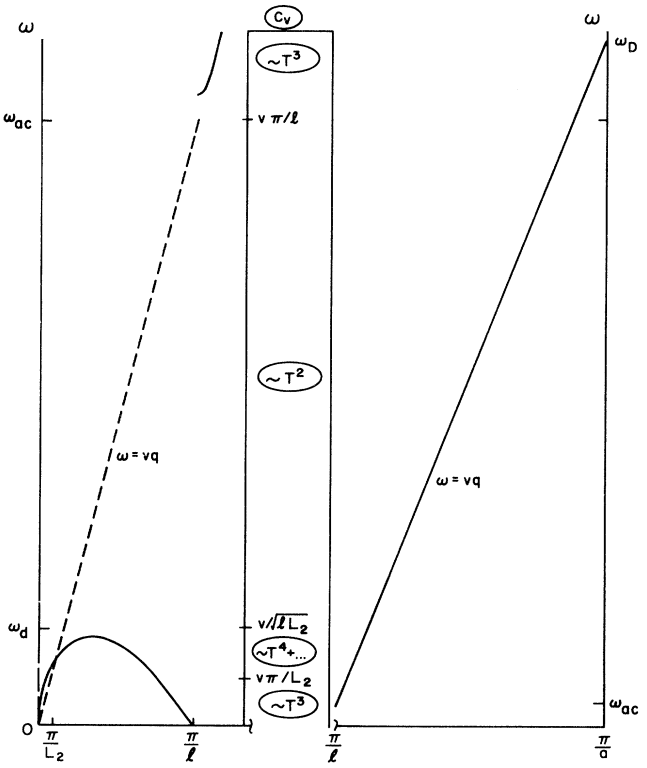

FIG. 8. Dyadon spectrum with the rest of the acoustic branch (schematic); note different scales on left and right. Dashed part collapses to the lower dyadon branch in the presence of twin boundaries. At $q=\pi/l$ the upper branch is curved in a range $\sim 1/\xi$ of q. The middle section shows (circled) the temperature dependence of the specific heat in various temperature regimes which correspond to the marked characteristic frequencies.

is bent periodically with a wave vector q_2. This mode involves strains within the product phase which extend away from the twin boundary. The volume that these strains occupy is of the same order as that for the related kinetic energy. Thus, unlike the case of flat translations, the restoring force for the $q_2 \neq 0$ modes acts in the same volume as their kinetic energy; hence we expect the usual $\omega \sim q_2$ dispersion. This can also be seen from Eqs. (14) and (19) by replacing $\eta(q_1)$ with $\eta(\mathbf{q})\exp(iq_2 r)$ and renaming the previous q as $q_1 (|q_1| < \pi/l)$:

$$u(s,r) = u_0(s) + \frac{2i\epsilon}{l} \sum_{p,\mathbf{q}} \frac{e^{iq_1 l} - 1}{q_1 + (2\pi/l)p} e^{i(q_1 + 2\pi p/l)s + iq_2 r} \eta(\mathbf{q}) + O(\eta^2) , \tag{25}$$

where $u_0(s)$ is the static solution. A typical elastic energy associated with the $\partial u/\partial r$ strain is then

$$\alpha_2 \int\int dr\, ds \left[\frac{\partial u}{\partial r} \right]^2 = \alpha_2 \epsilon^2 L_1 L_2 \sum_{\mathbf{q}} q_2^2 \eta(\mathbf{q})\eta(-\mathbf{q}) , \tag{26}$$

where $\sum_p (x-p)^{-2} = \pi^2/\sin^2 \pi x$ was used. We conclude then that the three-dimensional dyadon dispersion has the form

$$\omega^2(\mathbf{q}) = \omega^2(q_1) + v_2^2 q_2^2 + v_3^2 q_3^2 , \tag{27}$$

with v_2, v_3 of the order of usual sound velocities.

It is interesting to evaluate the magnitude of thermal fluctuations of a twin boundary, which for the harmonic Hamiltonian at temperature T are given by

$$\langle \delta S^2 \rangle = \epsilon^2 \sum_{n=1}^{M} \langle \delta_n^2 \rangle / M = \frac{8kT}{\rho} \int \frac{d^3 q}{(2\pi)^3} \frac{\sin^2(\frac{1}{2} q_1 l)}{\omega^2(\mathbf{q})} . \tag{28}$$

Using Eq. (27) and replacing $\omega(q_1) \simeq \omega_d$, we obtain

$$\frac{\langle \delta S^2 \rangle}{a^2} = \frac{kT}{\pi \alpha_\perp a^3} \frac{a}{l} \ln \left[\frac{\pi^2 l L_2}{ac} \right] , \tag{29}$$

where $\pi/a, \pi/c$ are cutoffs of the q_2, q_3 integrations, respectively, and $v_2 \simeq v_3 \simeq (\alpha_\perp/\rho)^{1/2}$. For $YBa_2Cu_3O_7$, we estimate $\alpha_\perp a^3 \simeq 16$ eV, $l/a \simeq 30$, $L_2/c \simeq 300$, so that at room temperature $(\langle \delta S^2 \rangle / a^2)^{1/2} \simeq 0.01$, and for In-Tl about 0.001, very small fractions of a lattice constant! [Note that Eq. (28) describes the thermal mean-square amplitude of the *atomic* displacements; the actual positions of the twin boundaries fluctuate more strongly by a factor ϵ^{-1} [Eq. (11)]. Hence thermal fluctuations have a weak effect on the coherency of twin boundaries, a coherency which should be observable in a variety of experiments, as discussed in the next section.

IV. EXPERIMENTAL PROBES

Twin boundaries are easily seen in optical or electron microscopy. Hence their static properties such as relative orientation, spacing, and width, as derived in Sec. II, can be experimentally determined. To our knowledge the dynamic behavior of twin boundaries has not been studied, so far, and in this section we discuss some possible methods, viz., elastic vibrations and waves, scattering experiments, specific heat, and electrical resistivity.

The methods commonly in use for the measurement of elastic constants, viz., resonance techniques and traveling-wave methods could, in principle, be adapted to verify experimentally the theoretically derived dyadon dispersion relation [Eq. (21)], but would, in addition to the measurement of resonance frequency or travel time, require the independent and more difficult determination of the wavelength of the dyadon excitation. For the case of standing waves the *modulation* of the twin-boundary spacing could be measured by means of optical reflection microscopy, but would still require a sufficient increase in experimental resolution. For a typical transformation strain of a few percent, large (transverse) atomic displacement in the order of tens of nanometers would be required in order to produce twin-boundary displacements comparable to the wavelength of light.

Alternatively, it seems feasible to excite individual standing dyadon modes in a suitable uniformly twinned crystal electrostrictively by depositing a thin layer of a highly electrostrictive material on the twin-relief corrugated face of the twinned-product phase region opposite to the habit plane and (by means of a pulsed tunable infrared laser or microwave maser) setting up a polarized standing electromagnetic wave with wave vector parallel to the twin-boundary normal (Fig. 10). Under resonance conditions the pulse frequency and the (optical or microwave) wavelength then determine the frequency and wavelength of the excited dyadon mode. The stress induced in the twin-band electrostrictively is described by a modulation σe^{iks}, which couples to the strain via the coupling energy:

$$E_c = \sigma \int_{S_0}^{S_M} e^{iks} \left[\frac{\partial u}{\partial s} \right] ds . \tag{30}$$

By a partial integration this involves the Fourier transform of $u(s)$ [Eq. (14)]. Hence

$$E_c = 2\sigma\epsilon M(e^{-iql} - 1)\eta(q') + O(\eta^2) , \tag{31}$$

with q' the reduced wave vector $q' = q + 2\pi p/l$, $|q'| < \pi/l$. The coupling becomes weaker as $q' \to 0$.

A scattering experiment, either by light or by neutrons, involves the lattice sum

$$\sum_n e^{iq(na+u)} \simeq \sum_n e^{iqna} + iq(Ml/a)u(q) + O(u^2) , \tag{32}$$

where a is a lattice constant. Here the coupling $qu(q)$ is of the same form as in Eq. (31). Note that in both cases the relation $q' = q + 2\pi p/l$ allows some flexibility in the choice of wave vector. The more serious constraint is to look for frequencies in the technically difficult range of $10^9 - 10^{11}$ sec^{-1}. Thus, while inelastic neutron scattering would be only marginally possible, Brillouin and laser Raman scattering (including second order) seem to be more promising.

Next, we consider the specific heat C_v due to dyadon

excitations. In view of the gap in the spectrum $\omega(q_1)$ and the extreme anisotropy of dyadons, we expect four qualitatively different regimes for the temperature dependence of C_v (Fig. 8).

(a) $T < v\pi/L_2 \simeq \omega_D a/L_2$, where v is a typical sound velocity, a is a lattice constant, and $\omega_D = v\pi/a$ is the Debye frequency. In this regime thermally excited waves with $vq < T$ cannot be confined in the product phase and the normal dispersion $\omega \sim q$ should result in all directions. Hence, in this regime, $C_v^{(1)} \sim T^3$.

(b) $v\pi/L_2 < T < \omega_d \simeq v\pi/(lL_2)^{1/2}$. In this regime dyadons are thermally excited and $C_v(T)$ depends on the detailed form of $\omega(\mathbf{q}_1)$. The most peculiar contribution comes from the $\omega \sim \sqrt{q_1}$, regime: Temperature imposes a cutoff on q_1, which is $\sim T^2$, while in the other directions q_2 and q_3 can be exited up to $\sim T/v$; hence $C_v^{(2)} \sim T^4$ plus other terms.

(c) $\omega_d < T < v\pi/l \simeq \omega_D a/l$. In this regime all the frequencies $\omega(q_1)$ are excited and the cutoff on the q_1 phase space is temperature independent, $q_1 \leq \pi/l$. Thus only the excitations with q_2 and q_3 are temperature limited and C_v is effectively two dimensional, i.e., $C_v^{(3)} \sim T^2$.

(d) $v\pi/l < T$. Here the acoustic modes with $|q_1| > \pi/l$ contribute again. Except very near $q_1 = \pi/l$, the dispersion of these modes should be linear; hence $C_v^{(4)} \sim T^3$.

We have evaluated numerically $C_v(T)$ via

$$C_v = \frac{\partial}{\partial T} \int \frac{d^3q}{(2\pi)^3} \frac{\omega(\mathbf{q})}{e^{\omega(\mathbf{q})/T} - 1} , \tag{33}$$

with $\omega(\mathbf{q})$ from Eqs. (21) and (27). Figure 9 shows the result (full line) and is compared to a system without twins, i.e., with usual acoustic modes (dashed line). In the actual system C_v should interpolate from the full line at low T to the dashed line at higher T, i.e., passing from regime (c) to (d). The full line in Fig. 8 can be fitted with

$$C_v \simeq 7T^2/(2\pi v^2 l) , \tag{34}$$

with deviations only at very low temperature, $T < 0.1\omega_d$ [regime (b)]. Comparing the dashed line of Fig. 9, for which $C_v = 2\pi^2 T^3/(5v^3)$, with Eq. (34) defines a crossing temperature

$$T_x \simeq 0.1\omega_{ac} = 0.1\omega_D a/l . \tag{35}$$

For $T > T_x$, we expect $C_v \sim T^3$, while for $T < T_x$, C_v of a twinned sample is enhanced relative to that of the untwinned one and behaves as $C_v \sim T^2$.

For In-Tl, $\omega_D \simeq 300$ K, $a/l \simeq 10^{-3}$, and $T_x \simeq 0.03$ K. In $YBa_2Cu_3O_7$, $\omega_D \simeq 400$ K, and $l/a = 25$–250 so that $T_x = 1.6$–0.16 K. Experimental data are referred to below.

Finally, we consider the metallic resistivity ρ_e due to electron-dyadon coupling. In general, a linear temperature dependence $\rho_e \sim T$ is due to electron-phonon scattering[18] and is valid above $\sim \omega_D/3$, where a Bose factor is approximated as $N(\omega_q) \simeq T/\omega_q$. Since the typical dyadon frequency is $\omega_d \ll \omega_D$, we expect this $\rho_e \sim T$ dependence to persist at much lower temperatures when an electron-dyadon coupling is present.

Equation (14) shows that electrons which would ordinarily couple to a phonon displacement $u(\mathbf{q})$ with a coupling constant $g_0(\mathbf{q})$ will then couple to the dyadon normal modes $\eta(\mathbf{q})$ with a coupling

$$g_d(\mathbf{q}) = ig_0(\mathbf{q})(e^{iq_1 l} - 1)/(q_1 l) . \tag{36}$$

We define a dimensionless coupling by a two-dimensional average:

$$\lambda_d(q_1) = (2/\pi v_F) \sum_{q_2, q_3} |g_d(\mathbf{q})|^2/\omega(\mathbf{q}) , \tag{37}$$

where v_F is a Fermi velocity in the q_1 direction. For $|q_1| < \pi/l$ the coupling $\lambda_d(q_1) \simeq \lambda_d(0) \equiv \lambda_d$ is weakly dependent on q_1, but for $|q_1| > \pi/l$ it decreases rapidly [Eq. (36)]. In view of the low frequencies in $\omega(\mathbf{q})$, we expect from the *two*-dimensional average (Eq. 37) that $\lambda_d > \lambda_0$, where λ_0 is the conventional coupling,[18] i.e., the three-dimensional average of $|g_0(\mathbf{q})|^2/\omega_{\mathbf{q}}$. Note, however, that λ_d is effective in a reduced phase space $|q_1| < \pi/l$.

Analogous to the electron-phonon formalism,[18] the electron-dyadon contribution to the resistivity is

$$\rho_e(T) \simeq 2\pi m^*(a/l)\lambda_d T/(e^2 n) , \tag{38}$$

where m^* and n are the electron effective mass and density, respectively, and the factor a/l accounts for the reduced phase space.

We note that some of the high-T_c superconducting compounds exhibit a linear $\rho \sim T$ dependence down to unexpectedly low temperatures, in fact down to T_c. Thus, in $YBa_2Cu_3O_7$, $\rho_e \sim T$ down to ~ 90 K, while in doped La_2CuO_4, $\rho \sim T$ down to 40 K;[19,20] in both cases this is well below $\omega_D \simeq 400$ K.

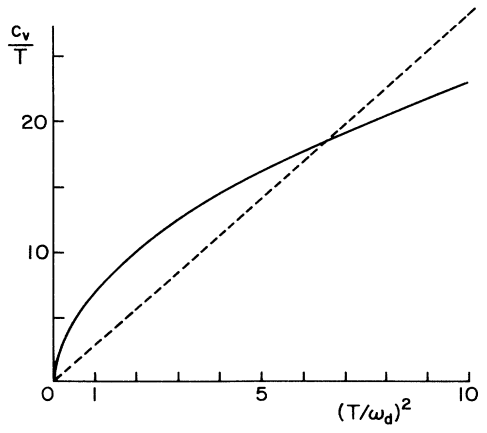

FIG. 9. Specific heat C_v due to dyadon excitations (solid line) in units of $\omega_d/(2\pi v_2 v_3 l)$. The dashed line shows C_v for a normal acoustic mode with $v = v_2 = v_3$ and $L_2/l = 100$.

V. DISCUSSION

The crucial role which the strain energy associated with the parent–twinned-product interface plays in the kinetic and morphology of martensitic transformation has been recognized for a long time; it has not only led to the geometric theory of the invariant plane strain,[12] but

has even been proposed as the generic criterion for martensitic transformations.[21] In spite of this importance most theoretical work on the subject deals only with the static elastic properties of a variety of pertinent geometric configurations.[1–3,13] In the present work it has therefore been our goal to study the elementary excitations of a martensitic twin band that is stabilized by the elastic interaction with the (austenite) parent phase across the habit plane. As a prerequisite, it was necessary to rederive the result for the relation $l \sim \sqrt{L_2}$ between twin spacing l and width L_2 of a twin band given by Khachaturyan and Shatalov[13] independently from a different perspective. The main new result is the dispersion relation given in Eqs. (21) and (22) for the collective twin-boundary oscillations ("dyadons") and the associated normal modes [Eqs. (18) and (19)] describing displacement waves which correspond to longitudinal twin-boundary motion; their consequences for several physical and materials properties have been discussed in Sec. IV.

The approach taken consists of using linear elasticity theory for the parent phase in conjunction with the *assumption* of a sawtooth displacement profile (i.e., $\xi \ll l$) for the twinned-product phase which imposes the boundary conditions on the parent phase at the habit plane. The *physical* parameters of the static model are the components of the elastic constant tensor in the parent phase, plus the transformation ("Bain") strain and the formation energy E_0 for the twin boundaries in the product phase. In addition, the dyadon frequencies are proportional to $\rho^{-1/2}$ (ρ the mass density).

In writing the second half of Eq. (10) and in deriving Eqs. (21) and (22), we have tacitly assumed a *proper* ferroelastic. Although for an *improper* ferroelastic the primary order parameter does not represent the shape change characteristic of martensitic transformations, this does not affect the elastic energy associated with the habit plane. The only changes required in this case are that the twin-boundary energy E_0 must be calculated separately on the basis of an appropriate Landau-Ginzburg model, and that the kinetic energy of the primary order parameter must be added to the elastic kinetic energy of a moving twin boundary. However, since the former is proportional to the twin-boundary width, it should be negligible for $\xi \ll l$. Therefore, the functional form $l \sim \sqrt{L_2}$ [Eq. (10)] and the dyadon dispersion relation ω/ω_d versus q [Eq. (21)] are valid for both *proper* and *improper* ferroelastic martensites.

In view of our understanding of the statics and dynamics of twin boundaries, we discuss now the properties of two representative materials: In-Tl with wide twin boundaries $\xi \gg a$, and $YBa_2Cu_3O_7$ (Y-Ba-Cu-O) with $\xi \simeq a$. We have inferred the ξ/a ratio from the static energy considerations via Eq. (10). For Y-Ba-Cu-O, ξ is also known directly[11] and agrees with our estimate; we are not aware of similar data on In-Tl.

The ratio ξ/a is of great significance for the dynamics, since the pinning energy in Eq. (23) can be neglected only for $\xi \gg a$. Thus, for Y-Ba-Cu-O, pinning may raise the dyadon frequencies, diminish the gap at $q = \pi/l$, and reduce the temperature range for which $C_v \sim T^2$. Experimental data on the specific heat of Y-Ba-Cu-O[22] can be fitted with a $C_v \sim T^2$ behavior plus $a \sim 1/T^2$ for possible Schottky defects. Other fits however are also possible.[22]

The In-Tl system is a better candidate for observing the unusual dynamics of twin boundaries since we expect $\xi \gg a$ and hence weak-pinning effects. Thus ultrasound and Brillouin scattering could probe the gap in the transverse acoustic mode for propagation perpendicular to the twin boundaries. We expect this gap to be in the range of 10^9–10^{10} $\sec^{-1}$. The specific heat should show a $\sim T^2$ term below ~ 0.3 K which becomes dominant below ~ 0.03 K.

We note that the unusual anisotropic dyadon dispersion may affect the superconducting transition temperature T_c.[9,23] The necessary ingredients for this are weak pinning of the twin boundaries (i.e., $\xi \gg a$) and matching anisotropy in the electron Fermi surface, i.e., planar sections parallel to the twin boundaries. Hence Y-Ba-Cu-O with $\xi \simeq a$ is not a good candidate. Some low-T_c elements such as Sn, Nb, and others have in fact shown a localized T_c enhancement near twin boundaries.[24] The presence of dyadons in these system and their possible effect on T_c can and should be tested by further experiments.

Finally, the feasibility of observing dyadons and other applications raises the question of their damping, i.e., attenuation. We have not yet developed the necessary theory to provide quantitative estimates. On the other hand, we believe from phenomenological arguments, and existing experimental data, that even near the transition temperature, where damping is of more concern, there is reason for optimism.

It is essential to reemphasize that the motion of a twin boundary via a topological strain soliton is completely different from the oscillation of an edge dislocation. The former is simply a nonlinear, local small-amplitude displacement wave (cf. end of Sec. III) rippling through the lattice, neither requiring nor producing defects (e.g., dislocations, vacancies). The latter, by contrast, involves vacancy jumps, intrinsically yielding strong phonon emission and attenuation. Heuristically, therefore, we may expect the damping of dyadons to be less (very much!) than that of dislocation oscillations.

Turning to the experimental situation, extensive ultrasonic measurements have been carried out on $A15$ martensitic intermetallic compounds and other (proper and improper) ferroelastics.[25–29] "Large" attenuation effects are attributed to domain-wall motion in the martensitic phase, and even to precursors before the transformation.[30,31] Upon approaching the transition temperature from above for the [110]/[110] TA mode in V_3Si and In-Tl alloys (which have the same symmetry as the dyadon modes), the attenuation is even too large to be measured by standard ultrasonic echo techniques.[27,28]

The issue, however, is how large is "large." As usually discussed, it is implicitly taken with respect to good metals, $Q = \omega/\Delta\omega \sim 10^5$. But that is not the point; the concern here is whether $Q < 1$, i.e., whether the mode is overdamped. In that context we refer to the results of Snead and Welch[26] and of Testardi and Bateman[27] who measured ultrasonic decrements and attenuation, attributed to domain-wall motion, from kHz to 10^2 MHz. From the relation[32] $Q \simeq \pi/\lambda\alpha$ [where λ = wavelength and α = ul-

trasonic attenuation (in Np/unit length), valid for $Q \gg 1$], one estimates from the experimental attenuation data of Testardi and Beteman for V_3Si [Figs. 2 and 3 of Ref. 27] for [100] LA modes at 4.5 K and 400 MHz ($\lambda = 20\ \mu$m) a quality factor of $Q \simeq 1400$. For the (highly attenuated!) [110]/[110] TA modes at 30 K and 60 MHz ($\lambda = 11\ \mu$m), one obtains $Q \simeq 1700$. Taking the frequency dependence as[27] $\alpha \sim \omega$, this extrapolates (at 30 K) to values of $Q \simeq 250$ and 25 at 400 MHz and 4 GHz, respectively. Testardi and Bateman[27] find that for the soft [110]/[110] TA branch above the phase transition $\alpha \sim v^{-3}$ (v the sound velocity), in agreement with theoretical models,[33] i.e., that the rapid increase of α for this mode with decreasing temperature does not primarily arise from an increase in the relaxation time, but from the softening of the shear modulus (C_{11}-C_{12}). Consequently, one may expect smaller α values and larger Q values for martensites with less shear-modulus softening, i.e., for those that show more strongly first-order transitions.

While both ultrasonic attenuation and resonance experiments (as proposed in Fig. 10) probe the relaxation time of the elementary excitations away from thermal equilibrium that are produced by an external perturbation, in scattering experiments (i.e., as proposed here, specifically Brillouin scattering) the Q factor is determined by the imaginary part of the (in the present case, dyadon) self-energy arising from anharmonic dyadon-phonon interactions. Although there is no experimental evidence for this quantity, there is no reason to expect the dyadon modes to be overdamped (except in those relatively rare cases where the soft mode itself is overdamped). *In particular,* well below the structural transition temperature (where our collective mode description is valid), damping at $q \to 0$ should vanish as ω^2, as for conventional transverse-acoustic modes.[33,34] The damping of the modes near $q = \pi/l$ is less certain, since these modes are sensitive to pinning by defects.

From these estimates it would seem that, if the TB motion is just dyadon oscillation, the dyadons are far from being overdamped and could well be observable in the kind of resonance experiment proposed in Fig. 10. A formal theory of TB domain-wall motional damping has not been developed to any significant degree, perhaps for lack of a manageable formal description of twin-boundary and martensitic structures. From the present model it now stands as a challenge to answer such questions, adding anharmonic coupling to phonons, interactions with defects, and finite-temperature considerations. These present a formidable task.

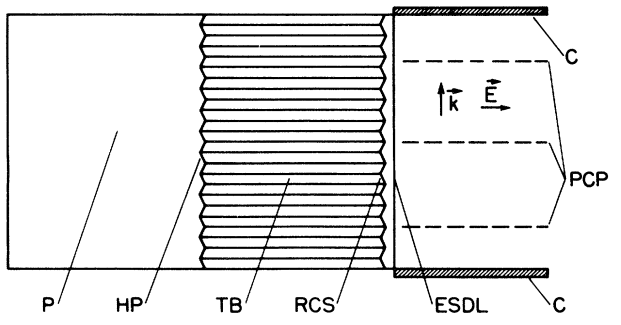

FIG. 10. Proposed experimental configuration for measurement of dyadon dispersion (front view; schematic). *P*, parent phase; HP, habit plane; TB, twin band; RCS, relief-corrugated surface of twinned-product phase; ESDL, electrostrictive dielectric layer; *C*, optical or microwave cavity; **k**, **E**, and PCP, wave vector, electric field, and planes of constant phase, respectively, of pulsed monochromatic-polarized standing electromagnetic wave.

ACKNOWLEDGMENTS

This work was supported by the U.S. Department of Energy under Grant No. DE-FG02-85ER45214 to the Pennsylvania State University and under Grant No. DE-FG02-88ER45364 to Cornell University. One of us (B.H.) is thankful for the hospitality of the Laboratory of Atomic and Solid State Physics, Cornell University, Ithaca, NY.

APPENDIX A: HABIT-PLANE ORIENTATION FOR A *T-O* TRANSITION

Consider a tetragonal system with coordinates $\mathbf{R} = (r,s,z)$ rotated by 45° relative to the axes x_i of the primitive cell, i.e., $r = (x_1 - x_2)/\sqrt{2}$, $s = (x_1 + x_2)/\sqrt{2}$, and $z = x_3$: An orthorhombic system is generated by the displacement[5]

$$\mathbf{u} = (\pm \epsilon s, 0, 0) , \tag{A1}$$

and the $\pm$ signs refer to the two possible twins. The allowed boundary between these twins is the (0,1,0) plane, i.e., $s = 0$. The sites $\mathbf{R}'$ of the transformed system are given by $\mathbf{R}' = \mathbf{R} + \mathbf{u} = B\mathbf{u}$, where B is the Bain strain. For the two twins we have $B = B_1$ and $B = B_2$, respectively, where

$$B_1 = \begin{bmatrix} 1 & \epsilon & 0 \\ 0 & 1 & 0 \\ 0 & 0 & 1 \end{bmatrix}, \quad B_2 = \begin{bmatrix} 1 & -\epsilon & 0 \\ 0 & 1 & 0 \\ 0 & 0 & 1 \end{bmatrix} . \tag{A2}$$

The corresponding strains are[5] (including geometric nonlinearity) $e_1 = \epsilon^2/2\sqrt{2}$, $e_2 = \epsilon/\sqrt{2}$, and $e_3 = -\epsilon^2/4$. To lowest order, e_2 defines the transition and is therefore its order parameter. We note that other choices of describing the *T-O* transition can differ from the above by $O(\epsilon^2)$ terms. The result for the habit plane may depend on this choice.

The normal $\mathbf{m} = (0,1,0)$ is not affected by the transformation [i.e., $(B_1^{-1})^{\dagger}\mathbf{m} = (B_2^{-1})^{\dagger}\mathbf{m} = \mathbf{m}$]. Hence there is no need for a rotation to match the twins at the twin boundary, as in other cases.[2]

Consider next a TBL whose volume fraction of twins of type 1 is $\frac{1}{2}(1+\delta)$ and of type 2 is $\frac{1}{2}(1-\delta)$. The asymptotic $\mathbf{R} \to \infty$ transformation is determined by the average

$$\langle A \rangle = \tfrac{1}{2}(1+\delta)B_1 + \tfrac{1}{2}(1-\delta)B_2 . \tag{A3}$$

The habit plane (or the invariant strain plane) is defined as a plane for which $\langle A \rangle$ is at most a rigid rota-

tion $\hat{\mathbf{R}}_1$. This plane can then be matched to the parent phase with no diverging strain energies. The usual construction[2,12] is to find a transformation over *all* space which allows for displacement gradients only in one direction $\mathbf{n}$ in addition to a rotation $\hat{\mathbf{R}}_1$; $\mathbf{n}$ then defines the habit plane. We find that for the present case it is much simpler to look for a plane defined by $\mathbf{R}=(-s\tan\theta,s,z)$ (see Fig. 2) for which we solve directly $\langle A\rangle\mathbf{R}=\hat{\mathbf{R}}_1\mathbf{R}$, i.e.,

$$\begin{bmatrix}1 & \delta\epsilon & 0\\ 0 & 1 & 0\\ 0 & 0 & 1\end{bmatrix}\begin{bmatrix}-s\tan\theta\\ s\\ z\end{bmatrix} = \begin{bmatrix}\cos\phi & -\sin\phi & 0\\ \sin\phi & \cos\phi & 0\\ 0 & 0 & 1\end{bmatrix}\begin{bmatrix}-s\tan\theta\\ s\\ z\end{bmatrix}, \quad \text{(A4)}$$

where ϕ defines the rotation matrix $\hat{\mathbf{R}}_1$. Equation (A4) must be valid for all s,z, which easily yields

$$\tan\theta=\tfrac{1}{2}\delta\epsilon\ , \quad \text{(A5)}$$

$$\sin\phi=-4\delta\epsilon/(4+\delta^2\epsilon^2)\ . \quad \text{(A6)}$$

The case $\delta=0$, i.e., equal sizes of twins 1 and 2, is special in that $\theta=0$ is independent of the strain ϵ. It is also special since $\phi=0$; i.e., a relative parent-product rotation is not necessary. If during the transformation the boundary conditions of the whole system (parent+product phase) are fixed, then $\phi=0$ is required. This yields the choice $\delta=0$ in Sec. II, which then implies the periodic condition on $u(s)$ of Eq. (11).

APPENDIX B: PARENT RESPONSE IN THE *T-O* TRANSITION

We model a *T-O* transition by a two-dimensional displacement field $(w_1,w_2,0)$, which depends on the coordinates r,s; if x_i are axes of the primitive tetragonal cell, then $r=(x_1-x_2)/\sqrt{2}$ and $s=(x_1+x_2)/\sqrt{2}$; also w_1,w_2 are components in the r and s directions, respectively. Linear elasticity then involves three elastic constants A_1, A_2, A_3 with static equations[5]

$$\begin{aligned}A_1\left[\frac{\partial^2 w_1}{\partial r^2}+\frac{\partial w_2}{\partial r\,\partial s}\right]+A_2\left[\frac{\partial^2 w_1}{\partial s^2}+\frac{\partial^2 w_2}{\partial r\,\partial s}\right]\\ +\frac{1}{2}A_3\left[\frac{\partial^2 w_1}{\partial r^2}-\frac{\partial^2 w_2}{\partial r\,\partial s}\right]=0\ ,\\ A_1\left[\frac{\partial^2 w_1}{\partial r\,\partial s}+\frac{\partial^2 w_2}{\partial s^2}\right]+A_2\left[\frac{\partial^2 w_1}{\partial r\,\partial s}+\frac{\partial^2 w_2}{\partial r^2}\right]\\ -\frac{1}{2}A_3\left[\frac{\partial^2 w_1}{\partial r\,\partial s}-\frac{\partial^2 w_2}{\partial s^2}\right]=0\ .\end{aligned} \quad \text{(B1)}$$

Using the geometry of Fig. 2, we look for solutions of the form

$$\begin{aligned}w_1(r,s)&=\sum_k w_1(k)\exp[(ik\sin\theta+q\cos\theta)r\\ &\qquad +(ik\cos\theta-q\sin\theta)s]\ ,\\ w_2(r,s)&=\sum_k w_2(k)\exp[(ik\sin\theta+q\cos\theta)r\\ &\qquad +(ik\cos\theta-q\sin\theta)s]\ ,\end{aligned} \quad \text{(B2)}$$

which are periodic in y and decay as $x\to-\infty$ if $\mathrm{Re}\,q>0$ (see Fig. 2). Substituting (B2) in (B1) yields equations for $w_1(k),w_2(k)$, which have nontrivial solutions if the determinant of their coefficients vanishes. This yields

$$\begin{aligned}&[(A_1+\tfrac{1}{2}A_3)(ik\sin\theta+q\cos\theta)^2+A_2(ik\cos\theta-q\sin\theta)^2][(A_1+\tfrac{1}{2}A_3)(ik\sin\theta-q\sin\theta)^2+A_2(ik\sin\theta+q\cos\theta)^2]\\ &\qquad=(ik\sin\theta+q\cos\theta)^2(ik\cos\theta-q\sin\theta)^2(A_1+A_2-\tfrac{1}{2}A_3)^2\ ,\end{aligned} \quad \text{(B3)}$$

which is equivalent to the condition $\det(T)=0$ from Eq. (2). For $\theta=0$ this yields

$$q^2=k^2\{2A_1(A_3-A_2)+A_2A_3\pm2[A_2A_3(A_3-2A_2)(A_1+A_2)]^{1/2}\}/[2A_2(A_1+\tfrac{1}{2}A_3)]\ , \quad \text{(B4)}$$

which for any choice of A_i has four real solutions, two of which have the required $q>0$. Equation (B1) determines then the ratio $w_1(k)/w_2(k)$ for each solution, and the matching to the product phase [Eq. (1b)] determines the $w_1(k)$ and $w_2(k)$ values and, in terms of $u(k)$, the TBL solution in the product phase.

The elastic energy density which corresponds to Eq. (B1) is

$$\begin{aligned}\mathcal{H}_{\rm el}=&\frac{1}{4}A_1\left[\frac{\partial w_1}{\partial r}+\frac{\partial w_2}{\partial s}\right]^2+\frac{1}{4}A_2\left[\frac{\partial w_1}{\partial s}+\frac{\partial w_2}{\partial r}\right]^2\\ &+\frac{1}{8}A_3\left[\frac{\partial w_1}{\partial\gamma}-\frac{\partial w_2}{\partial s}\right]^2\ .\end{aligned} \quad \text{(B5)}$$

Integrating (B5) over the parent phase yields the interface energy of Eq. (6). The details of the solution are not

essential since the argument below Eq. (6) is clearly valid, leading to

$$E_{\text{in}}=\alpha L_1 L_3 \sum_k |k||u(k)|^2 \ . \tag{B6}$$

The coefficient α is a function of A_1, A_2, A_3; unless one of the elastic constants A_i (or some linear combinations of them) happens to be very small, α is of the order of A_i.

These considerations apply equally well to $\theta \neq 0$ geometries. Thus, for $\theta=45°$, we obtain the four solutions

$$q=\pm\beta ik \pm k(1-\beta^2)^{1/2} \ , \quad \beta^2=\frac{2A_1(\frac{1}{2}A_3-A_2)}{A_3(A_1+A_2)} \ . \tag{B7}$$

Since $A_i>0$ [local stability of the parent phase requires $\mathcal{H}_{\text{el}}>0$ for all strains in (B5)], we have $\beta^2<1$ and 2 solutions with $\text{Re}q>0$. The route to Eq. (B6) follows as above.

[1] J. W. Christian, Metall. Trans. **13A**, 509 (1982).

[2] A. G. Khachaturyan, *Theory of Structural Transformation in Solids* (Wiley, New York, 1983).

[3] See, e.g., *Shape Memory Effects in Alloys,* edited by J. Perkins (Plenum, New York, 1975).

[4] G. R. Barsch and J. A. Krumhansl, Phys. Rev. Lett. **53**, 1069 (1984).

[5] G. R. Barsch and J. A. Krumhansl, Metall. Trans. **19A**, 761 (1988).

[6] F. Falk, Z. Phys. B **51**, 177 (1983).

[7] A. E. Jacobs, Phys. Rev. B **31**, 5984 (1985).

[8] G. R. Barsch, B. Horovitz, and J. A. Krumhansl, Phys. Rev. Lett. **59**, 1251 (1987).

[9] B. Horovitz, G. R. Barsch, and J. A. Krumhansl, Phys. Rev. B **36**, 8895 (1987).

[10] Webster's Third New International Dictionary (W. Benton, Chicago, 1966) defines "dyad" as two units treated as one.

[11] For reviews, see J. Electron Microsc. Technol. **8** (3) (1988).

[12] M. S. Wechsler, D. S. Lieberman, and T. A. Read, Trans. AIME **197**, 1503 (1953).

[13] A. G. Khachaturyan and G. A. Shatalov, Zh. Eksp. Teor. Fiz. **56**, 1037 (1969) [Sov. Phys. JETP **29**, 557 (1969)].

[14] A. Moore, J. Graham, G. K. Williamson, and G. R. Raynor, Acta Metall. **3**, 579 (1955).

[15] B. A. Auld, *Acoustic Fields and Waves in Solids* (Wiley, New York, 1973), Vol. 2, pp. 94–102.

[16] Yu. A. Kosevich and E. S. Syrkin, Akust. Zh. **34**, 113 (1988) [Sov. Phys. Acoust. **34**, 61 (1988)].

[17] A. R. Bishop, J. A. Krumhansl, and S. E. Trullinger, Physica D **1**, 1 (1980).

[18] P. B. Allen, T. P. Beaulac, F. S. Khan, W. H. Butler, F. J. Pinski, and J. C. Swihart, Phys. Rev. B **34**, 4331 (1986).

[19] T. Fujita, Y. Aoki, Y. Macno, J. Sakurai, H. Fukuba, and H. Fujii, Jpn. J. Appl. Phys. **26**, L368 (1987).

[20] M. Gurvitch and A. T. Fiory, Phys. Rev. Lett. **59**, 1337 (1987).

[21] M. Cohen, G. B. Olson, and P. C. Clapp, in *Proceedings of the International Conference on Martensite ICOMAT 79,* edited by W. S. Owen (MIT, Cambridge, MA, 1979), p. 1.

[22] H. B. Brom, J. Baak, A. A. Menovsky, and M. J. V. Menken, Synth. Met. **29**, F641 (1988), and references therein.

[23] B. Horovitz, Synth. Met. **29**, F575 (1989).

[24] For a review, see I. N. Khlyustikov and A. I. Buzdin, Adv. Phys. **36**, 271 (1987).

[25] B. Faucher, J. F. Bussiere, C. L. Snead, Jr., and M. Suenaga, in *Proceedings of the Seventh International Conference on Internal Friction and Ultrasound Attenuation in Solids, Lausanne, Switzerland, 1981,* edited by W. Benoit and G. Gremaud [J. Phys. (Paris) Colloq. **42**, Suppl. 10, C5-1091 (1981)].

[26] C. L. Snead, Jr. and D. O. Welch, in *Proceedings of the Eighth International Conference on Internal Friction and Ultrasonic Attenuation in Solids, Urbana, Illinois, 1985,* edited by A. V. Granto, G. Mozurkewich, and C. A. Wert [J. Phys. (Paris) Colloq. **46**, Suppl. 12, C10-589 (1985)].

[27] L. R. Testardi and T. B. Bateman, Phys. Rev. **154**, 402 (1967).

[28] D. J. Gunton and G. A. Saunders, Solid State Commun. **14**, 865 (1974).

[29] K. Fossheim and B. Berre, Phys. Rev. B **5**, 3292 (1972).

[30] L. E. Tanner, A. R. Pelton, and R. Gransky, J. Phys. (Paris) Colloq. **43**, C4-169 (1982).

[31] N. Ohnishi, T. Onozuka, and M. Hirabayashi, in *Proceedings of the International Conference on Martensitic Transformations* (Japanese Institute of Metals, Sendai, Japan, 1987), p. 1127.

[32] A. S. Nowick and H. Berry, *Anelastic Relaxation in Crystalline Solids* (Academic, New York, 1972), p. 27.

[33] T. O. Woodruff and H. Ehrenreich, Phys. Rev. **123**, 1553 (1961).

[34] P. C. K. Kwok, Solid State Phys. **20**, 213 (1967).